

Magnetic anisotropy and switching process in diluted $\text{Ga}_{1-x}\text{Mn}_x\text{As}$ magnetic semiconductor films

Graeme P. Moore, Jacques Ferré,^{a)} and Alexandra Mougin

Laboratoire de Physique des Solides, UMR CNRS 8502, Bât. 510, Université Paris Sud, 91405 Orsay, France

Maria Moreno and Lutz Däweritz

Paul-Drude Institute of Solid-State Electronics, Hausvogteiplatz 5-7, 10117, Berlin, Germany

(Received 2 May 2003; accepted 24 June 2003)

Magnetic anisotropy and magnetization reversal phenomena are studied in $\text{Ga}_{1-x}\text{Mn}_x\text{As}$ films grown on GaAs(001). From the azimuthal dependence of the magneto-optical Kerr rotation and magnetic linear dichroism, the in-plane $\langle 100 \rangle$ directions are unambiguously assigned as axes of easy magnetization. The values of the cubic and uniaxial anisotropies are determined. Magnetization reversal proceeds by noncoherent spin rotation and irreversible jumps by formation of 90° domains.

© 2003 American Institute of Physics. [DOI: 10.1063/1.1601690]

I. INTRODUCTION

The discovery of ferromagnetism in Mn-containing III–V-based compounds^{1–3} has greatly attracted the attention of the magnetic and semiconductor research communities. In such compounds, ferromagnetism is mediated by charge carriers which have been found to be delocalized holes.⁴ In $\text{Ga}_{1-x}\text{Mn}_x\text{As}$ with $0.04 < x < 0.06$, the manganese acceptors may compensate the As_{Ga} antisite deep donors present in the material, giving rise to p -type conduction with a low metallic conductivity. p – d hybridization and the Zeener double exchange mechanism give a ferromagnetic coupling between the localized manganese spins mediated by the charge carriers. The highest reported Curie temperature ($T_C = 110$ K) has been obtained for $x = 4.7\%$,⁵ and efforts are underway to achieve higher T_C values. The transport, magnetic, and optical properties of $\text{Ga}_{1-x}\text{Mn}_x\text{As}$ make this system very attractive for fundamental studies as well as for future applications in spin-electronics. Recently, large tunnel magnetoresistances have been reported, up to 75% at low temperature for single $\text{Ga}_{1-x}\text{Mn}_x\text{As}/\text{AlAs}/\text{Ga}_{1-x}\text{Mn}_x\text{As}$ junctions,⁶ and even up to 800% have been predicted for double AlAs-barrier $\text{Ga}_{1-x}\text{Mn}_x\text{As}$ heterostructures.⁷ In spite of the large interest surrounding $\text{Ga}_{1-x}\text{Mn}_x\text{As}$ and the whole family of diluted magnetic semiconductors based on III–V compounds, only crude magnetic measurements have been performed so far. Deeper information, especially on the magnetic anisotropy and magnetization reversal process, is required for optimizing future applications of III–V diluted magnetic semiconductors in spin-electronics.

$\text{Ga}_{1-x}\text{Mn}_x\text{As}$ layers grown on GaAs (001) substrates are under compressive strain. The lattice expands in the $[001]$ growth direction.⁸ Strain favors an in-plane axis of easy magnetization. This property was theoretically predicted for $\text{Ga}_{1-x}\text{Mn}_x\text{As}/\text{GaAs}$ (001) with high enough hole density in the magnetic layer.⁴ The axis of easy magnetization was predicted⁴ to fluctuate between the in-plane $\langle 100 \rangle$ and $\langle 110 \rangle$

directions when varying the degree of occupation of the hole sub-bands, which depends on the Mn concentration x . Differences in the Mn content probably explain the discrepancies on the in-plane orientation of the easy magnetization axis reported by different authors.^{6,7,9,10}

In this article, we report on the magnetic anisotropy of a $\text{Ga}_{0.957}\text{Mn}_{0.043}\text{As}$ film grown on GaAs (001). The magnetic anisotropy has been obtained from several crossed magneto-optical informations. Measurements of the longitudinal Kerr rotation (LKR) in longitudinal or transverse magnetic fields, linearly proportional to the magnetization, and of the magnetic linear dichroism (MLD) in light reflection, quadratically related to the magnetization, unambiguously show that the axes of easy magnetization are the in-plane $\langle 100 \rangle$ directions. The out-of-plane anisotropy has been also determined by polar Kerr rotation measurements.

II. EXPERIMENTAL DETAILS

The 603 nm- $\text{Ga}_{0.957}\text{Mn}_{0.043}\text{As}$ film was grown by molecular beam epitaxy at low temperature (LT) ($T \approx 272^\circ\text{C}$) on a 9 nm-thick predeposited LT-GaAs. The sample had a rectangular shape (7 mm \times 4 mm) with the long edge oriented along the $[1\bar{1}0]$ direction. The Curie temperature was measured to be 57 K.

LKR measurements were performed using a sensitive modulation magneto-optical technique.¹¹ Longitudinally p -polarized (p is in the plane of incidence) light is reflected by the film at the 45° angle of incidence. In order to analyze the state of polarization of the emergent beam, it passes through a photoelastic modulator (frequency $\Omega = 50$ kHz), through a second polarizer oriented at 45° with respect to the p -direction, and is finally detected by a photomultiplier. We used green light ($\lambda = 543$ nm), emitted by a He–Ne laser, to work far away from the $\text{Ga}_{1-x}\text{Mn}_x\text{As}$ band edge and to prevent spurious interference effects. The magnetic field is applied either in the longitudinal (L) or transverse (T) configurations, i.e., oriented in the plane of incidence of the light or perpendicular to it, respectively. Analogous notations, M_L

^{a)}Electronic address: ferre@lps.u-psud.fr

and M_T , hold for the magnetization components. To determine the normal magnetization component (M_P), the field is applied perpendicularly to the film plane, i.e., in the polar configuration. LKR is measured at the 2 Ω frequency. In azimuthal measurements the sample is rotated, by an angle φ , around the axis perpendicular to the film plane, either in the longitudinal (L) or transverse (T) field configurations.

MLD measurements were carried out at normal light incidence to avoid detection of LKR effect.¹² The magnetic field was applied in either the L or T configurations. The MLD measurements were performed using a photoelastic modulation technique, with the same optical elements as in LKR measurements.¹³ Alternatively s - and p -polarized (longitudinally and transversely polarized) incident light, at the 2 Ω frequency, was probed by a polarizer followed by a photoelastic modulator. The light reflected by the sample was finally detected by a photomultiplier. The experimental MLD signal is defined as two times the difference between the reflectivities in longitudinal (p) and transverse (s) polarized light divided by their sum.

III. RESULTS AND DISCUSSION

The total magnetic energy, E_{magn} in C_{4v} symmetry may be written as⁴

$$E_{\text{magn}} = K_u \cos^2 \theta + K_c (\sin^4 \theta \sin^2 \psi \cos^2 \psi + \sin^2 \theta \cos^2 \theta) \quad (1)$$

keeping only the lowest-order terms related to the cubic anisotropy coefficient K_c and grouping the strain-induced uniaxial effect and the dipolar contribution into a single term proportional to the uniaxial anisotropy coefficient K_u . Here, θ and ψ are the angles, in cylindrical coordinates, between the magnetization and the normal $[001]$ and in-plane $[100]$ axes, respectively. If $4K_u > -K_c$, Eq. (1) gives the in-plane (001) anisotropy energy. The easy axes are the $\langle 100 \rangle$ directions when $K_c > 0$, and the $\langle 110 \rangle$ directions in the opposite case. When the magnetization lies in the film plane ($\theta = 90^\circ$), Eq. (1) reduces to

$$E_{\text{magn}} = \frac{K_c}{4} \sin^2 2\psi. \quad (2)$$

The Zeeman term has to be included to account for the equilibrium positions of the magnetization as a function of the magnetic field and azimuthal angle ψ .

Let us assume that $4K_u > -K_c$ and $K_c > 0$, so that Eq. (1) gives the in-plane (001) anisotropy energy for axes of easy magnetization along $\langle 100 \rangle$ directions. As in Ref. 14, we suppose that the applied field is insufficient to produce uniform rotation of the magnetization away from the easy axes ($H \ll 2K_c/M$), but that after nucleation, the field component along the easy axes acts to move walls of 90° domains continuously in an incoherent way.

If the magnetic field is applied along a direction making an angle φ ($0 < \varphi < \pi/4$) with the $[100]$ axis (Fig. 1), on an initial magnetic state with spins aligned along the $[\bar{1}00]$ axis, two successive magnetization jumps are expected to occur when increasing the field from $-H_S$ to H_S (H_S being the saturation field). The first magnetization jump is related to

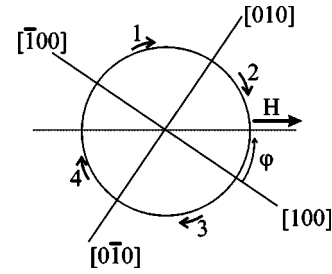


FIG. 1. Sketch of the magnetization reversal process when increasing the field H from $-H_S$ to H_S (H_S being the saturation field) along a direction making an angle φ with the $[100]$ axis. The axes of easy magnetization are assumed to be the in-plane $\langle 100 \rangle$ directions. Starting from a negative saturated state along $[\bar{1}00]$, the spins reorient to $[100]$ in a positive field, after a two-jump (1 and 2) clockwise process. Jumps 3 and 4 take place in a negative field.

the sudden appearance of large domains whose spins are oriented along the $[010]$ axis (Fig. 1), at the field

$$H_{c1} = \frac{\varepsilon}{M(\cos \varphi + \sin \varphi)} = \frac{\varepsilon}{\sqrt{2}M \sin(\varphi + \pi/4)}, \quad (3)$$

where ε is the nucleation pinning energy of 90° domains.¹⁴ A second magnetization jump occurs at a higher field

$$H_{c2} = \frac{\varepsilon}{M(\cos \varphi - \sin \varphi)} = \varepsilon\sqrt{2}M \cos(\varphi + \pi/4) \quad (4)$$

when new domains with spins parallel to the $[100]$ direction nucleate (Fig. 1). When the magnetic field decreases, two symmetric magnetization jumps occur at $H_{c3} = -H_{c1}$ and $H_{c4} = -H_{c2}$, the magnetization pointing first towards $[0\bar{1}0]$ to finally orient itself along $[\bar{1}00]$ (Fig. 1). Note that in this case the magnetization rotates clockwise by 90° steps. For $\varphi = 0$ and $\varphi = \pi/4$, the situation is somewhat atypical. For $\varphi = \pi/4$, since H_{c2} diverges, only the first jump at $H_{c1} = \varepsilon/\sqrt{2}M$ can be observed. For $\varphi = 0$, two energy-degenerated magnetization jumps take place at the same field $H = H_{c1} = H_{c2} = \varepsilon/M$. Then, in a positive field, the magnetization jumps from $[\bar{1}00]$ to $[010]$ or $[0\bar{1}0]$ and finally to $[100]$. In the $0 \leq \varphi \leq \pi/4$ interval, the LKR amplitude varies according to a $\cos \varphi$ law, between ϕ_S for $\varphi = 0$ and $\phi_S/\sqrt{2}$ for $\varphi = \pi/4$.

Oppositely, in the case of a $\langle 110 \rangle$ easy magnetization axis, a similar analysis can be obtained, but then the second coercive field diverges at $\varphi = 0$ and $\varphi = \pi/2$, and not for $\varphi = \pi/4$.

The LKR depends linearly only on the longitudinal and polar (M_L and M_P) components of the magnetization. We measured LKR hysteresis loops in a longitudinal field for different azimuthal angles φ . As an illustration, LKR (H_L) loops are shown in Fig. 2 for selected values of φ . The theoretical shape of the LKR (H_L) and LKR (H_T) loops, assuming easy axes parallel to in-plane $\langle 100 \rangle$ directions far away from in-plane $\langle 100 \rangle$ ($\varphi \neq 0 + k\pi/2$), and $\langle 110 \rangle$ ($\varphi \neq \pi/4 + k\pi/2$) directions, the LKR (H_L) loops exhibit two jumps at fields H_{c1} and H_{c2} [Fig. 2(c)], consistently with the theoretical predictions [Figs. 3]. The azimuthal variations of

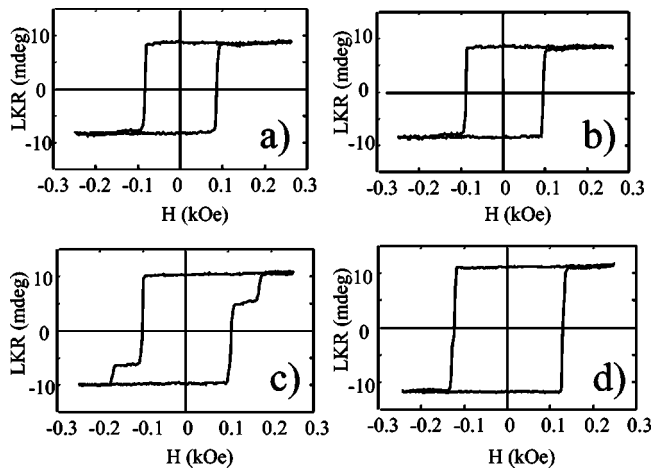


FIG. 2. LKR loops measured in a longitudinal field at 1.8 K for several azimuthal angles: (a) $\varphi \approx 45^\circ$, (b) $\varphi = 30^\circ$ (minor loop), (c) $\varphi = 15^\circ$, and (d) $\varphi \approx 0^\circ$.

H_{c1} and H_{c2} are depicted in Fig. 4. The experimental values of H_{c1} and H_{c2} in Fig. 4 are well fitted by Eqs. (3) and (4), implying that the two axes of easy magnetization lie along $\langle 100 \rangle$ directions. The measured LKR (H_L) maximum amplitude varies as $\cos \varphi$ in the $-\pi/4 < \varphi < \pi/4$ interval, which is also consistent with the assumption of easy axes parallel to in-plane $\langle 100 \rangle$ directions. The fact that the LKR value at saturation for longitudinal fields as large as 0.5 kOe equals the remnant LKR amplitude indicates that coherent spin rotation is negligible in small magnetic fields. This validates our assumption of $H \ll 2K_c/M$.

As expected, the LKR (H_L) coercivity is approximately $\sqrt{2}$ times higher for $\varphi = 0$ than for $\varphi = \pm \pi/4$ [see Figs. 2(a) and 2(d)]. In the case of a large nonequivalency between in-plane [100] and [010] anisotropy axes, two successive

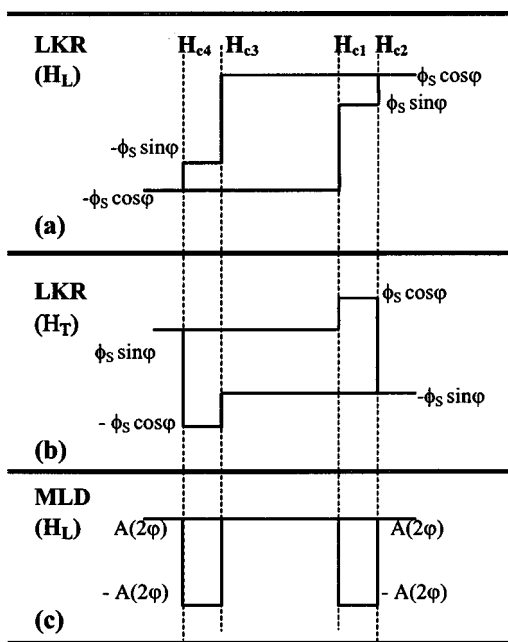


FIG. 3. Calculated (a) LKR (H_L), (b) LKR (H_T) and (c) MLD (H_L) loop shapes, for azimuthal angles in the range $0 < \varphi < \pi/4$.

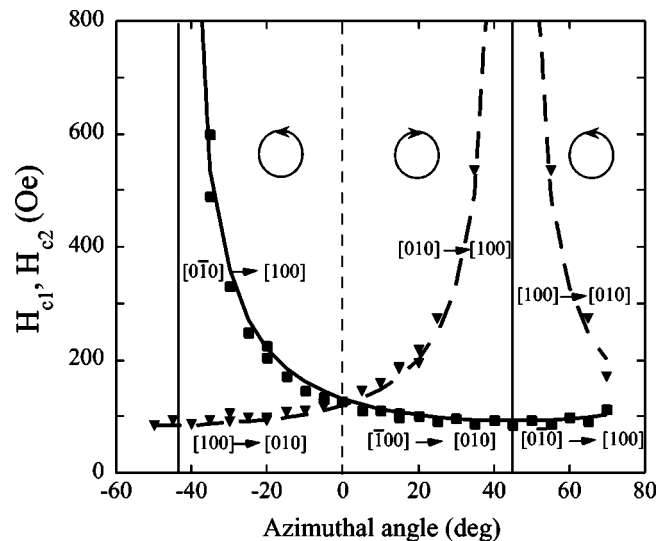


FIG. 4. H_{c1} (squares) and H_{c2} (triangles) azimuthal variations. The spin orientations of the domain states involved in the magnetization jumps and the spin rotation senses are indicated for each range of azimuthal angles.

jumps should occur at different field values for $\varphi = 0$ and $\varphi = \pi/2$. Only one jump in LKR amplitude is observed for fields applied along any of the in-plane $\langle 100 \rangle$ directions. Therefore, the [100] and [010] directions may be considered, in first approximation, as equivalent anisotropy axes.¹⁴ However, for $\varphi = +\pi/4$ and $\varphi = -\pi/4$, close but significantly different coercivities (85 Oe and 94 Oe, respectively) are measured. This means that there is a very small uniaxial in-plane anisotropy in the $\text{Ga}_{0.957}\text{Mn}_{0.043}\text{As}$ film, as recently reported in this material¹⁵ and in other systems.^{16,17}

When the temperature decreases, on one hand the coercive field strongly increases. For example, it increases from 64 Oe at 4.2 K up to 89 Oe at 1.4 K for magnetic fields applied along the [110] direction. This comes from the dynamics of the magnetization reversal process which strongly depends on temperature.¹⁸ On the other hand, the LKR value, proportional to the in-plane magnetization, as expected increases only by less than 5% upon such temperature decrease.

In a transverse magnetic field and for φ close to $\pi/4 + k\pi/2$, we could only measure minor LKR (H_T) loops, since the maximum available field was too low for reaching the second jump at H_{c2} (or H_{c4}) [Fig. 3(b)]. We found that the minor-loop LKR (H_T) amplitude varies with the azimuthal angle φ according to the expected $\phi = -\phi_S(\cos \varphi - \sin \varphi)$ law, in the $0 \leq \varphi \leq \pi/4$ interval. The LKR (H_T) amplitude vanishes for $\varphi = \pi/4$, but for $\varphi = 0$ or $\varphi = \pi/2$ a single jump from $-\phi_S/\sqrt{2}$ to $\phi_S/\sqrt{2}$ occurs. The independent measurements of LKR in longitudinal and transverse field configurations give consistent LKR signs with our calculations and the same value of 11.5 mdeg for ϕ_S .

We carried out complementary dynamical experiments giving insight into the magnetization reversal mechanism. For magnetic fields oriented along the [110] axis, the coercivity was found to vary by about 6 Oe per decade in the 20–500 Oe/s field sweeping rate range. This variation¹⁰ is a consequence of the magnetization reversal dynamics con-

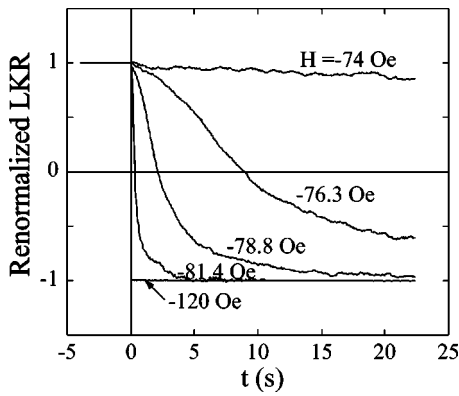


FIG. 5. LKR magnetic after-effect relaxation curves measured at 1.4 K, for different values of the applied longitudinal field, oriented along [110].

trolled by mechanisms of domain nucleation and wall propagation. We investigated the magnetization relaxation process—usually called the magnetic aftereffect—by looking at the LKR time dependence in a magnetic field parallel to the [110] direction.¹⁸ We measured relaxation curves by first saturating the sample in a positive field H_S and then applying a constant inverse field- H (see Fig. 5). The abruptness of the reversal is revealed by the sharp decrease of the characteristic relaxation time when the field H approaches the quasi-static coercive field value ($H_C = 85$ Oe). The negative curvature of the relaxation curves showing up at short times (see, for example the curve for $H = -76.3$ Oe in Fig. 5) indicates a mechanism of magnetization reversal by nucleation of 90° domains and fast domain wall motion.¹⁸ Such a mechanism is also evidenced on both jumps appearing in LKR loops [Fig. 2(c)]. Very recent high resolution magneto-optical imaging studies of the magnetic domain structure prove unambiguously such a reversal mechanism.¹⁹

We also investigated the second order magnetic linear dichroism (MLD) effect. The theoretical MLD (H_L) loop shape for a film of tetragonal symmetry and light propagation along its principal axis is that shown in Fig. 3(c), assuming easy axes oriented along in-plane $\langle 100 \rangle$ directions. The MLD depends on quadratic terms in magnetization components, i.e., M_L^2 , M_T^2 , and $M_L M_T$.^{12,13,17} The MLD (H_L) signal takes two opposite values $\pm A(2\varphi)$. From a general theoretical treatment,¹⁷ a detailed expression for $A(2\varphi)$ has been derived

$$A(2\varphi) = PM_L M_T + QM_L M_T \cos^2 2\varphi + R(M_L^2 + M_T^2) \sin 4\varphi$$

$$= P' \sin 2\varphi + Q' \sin 2\varphi \cos^2 2\varphi + R' \sin 4\varphi \cos 2\varphi,$$

(5)

where $P, Q, R,$ and P', Q', R' are φ -independent constants. The results of our MLD measurements (Fig. 6) are consistent with the theoretical predictions [Fig. 3(c)]. The MLD (H_L) signal vanishes for both $\varphi = 0$ and $\varphi = \pi/4$. For $\varphi = 0$, $A(2\varphi) = 0$, according to [Eq. (5)]. For $\varphi = \pi/4$, the two involved magnetization jumps (at H_{c1} and H_{c2}) are simultaneous, so that the MLD (H_L) signals associated to the jumps [$+A(\pi/4)$ and $A(\pi/4)$] cancel one another. The MLD (H_L) jumps take place at the same fields (H_{c1} and H_{c2}) as for LKR (H_L). We confirmed that the sign of the MLD (H_T)

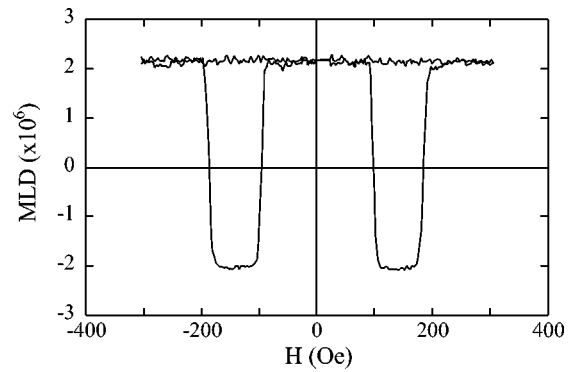


FIG. 6. MLD (H_L) hysteresis loop measured at 1.8 K for $\varphi = 16^\circ$. To achieve good signal-to-noise ratio, the loop recorded in 5 s has been measured 400 times and averaged. The MLD is defined by $[2(R_L - R_T)] / (R_L + R_T)$, where R_L and R_T are the film reflectivities for polarizations of the incident light parallel and perpendicular to the applied magnetic field, respectively.

signal in the transverse field is opposite to that of MLD (H_L) in the longitudinal field. The MLD measurements give independent proof that the in-plane $\langle 100 \rangle$ directions are here the easy magnetization axes.

In order to determine the K_u and K_c anisotropy constants, we measured the polar PKR (H_p) hysteresis loop in a field H_p oriented along the [001] direction, perpendicular to the film plane (Fig. 7). As previously reported,⁸ we found that the measured low-temperature PKR (H_p) loop is distorted. Oscillations due to optical interference effects are superimposed on the loop (Fig. 7). These oscillations can be averaged out to obtain the normalized perpendicular magnetization $m(H_p)$ loop. The loop shape is consistent with a hard axis perpendicular to the film surface, and in-plane cubic anisotropy.

If the remnant magnetization points towards one of the equivalent in-plane $\langle 100 \rangle$ axes, upon applying the field H_p the magnetization rotates coherently inside the $\{010\}$ plane containing the $\langle 100 \rangle$ axis. The total magnetic energy can be expressed as

$$E_{\text{magn}} = K_u \cos^2 \theta + \frac{K_c}{4} \sin^2 2\theta - MH_p \cos \theta$$

(6)

considering $\psi = 0$ in Eq. (1), and including the Zeeman term. Minimizing this expression with respect to θ , one finds

$$H_p = \frac{2m}{M^2} \left\{ K_u - K_c \left[2 \left(\frac{m}{M} \right)^2 - 1 \right] \right\}$$

(7a)

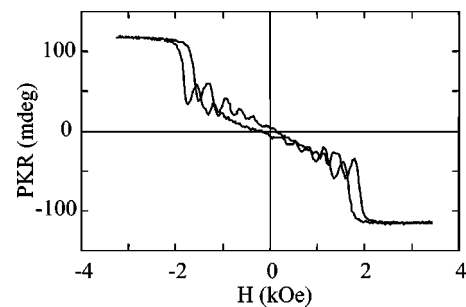


FIG. 7. PKR loop measured at 1.8 K.

$$\text{or } H_p = xh_u + h_c(x - 2x^3), \quad (7b)$$

where $x = m/M$ stands for the normalized component of the magnetization (i.e., the normalized Kerr signal) along the [001] direction and $h_u = 2K_u/M$ (respectively $h_c = 2K_c/M$) is the uniaxial (cubic) anisotropy field. The experimental data of Fig. 7 have been normalized (so $-1 \leq x \leq 1$) and are well fitted by Eq. 7(b), especially in the field range $|H| \leq 2000$ Oe where x varies linearly with the applied magnetic field. One finds $h_u = 3100$ Oe and $h_c = 1000$ Oe, with an error of about 20%. From independent magnetometry experiments (not shown), we obtain $M = 15$ emu/cm³ which implies $K_u = 2.32 \times 10^4$ erg/cm³ and $K_c = 0.75 \times 10^4$ erg/cm³. Thus, the uniaxial term is only about three times larger than the cubic anisotropy. While the value of K_u obtained here is consistent with other K_u determinations (e.g., a value $K_u = 2.9 \times 10^4$ erg/cm³ is given in Ref. 9 for $x = 3.5\%$), the ratio K_c/K_u has been previously often underestimated. For example, a value of 0.025 for K_c/K_u is given in Ref. 20. More pertinent anisotropy constants have been deduced from ferromagnetic resonance experiments in a sample with 3% of manganese;¹⁵ after a simple parameters conversion, those data lead to $h_u = 2700$ Oe and $h_c = 1000$ Oe, which is in perfect agreement with our above results.

The magnetization dynamics in Ga_{1-x}Mn_xAs epilayers look similar to that found in metallic magnetic films.¹⁸ The magnetized state looks perfectly homogeneous in spite of the alloyed (inhomogeneous) nature of the material. This is due to the far larger mean free path of the carriers in Ga_{1-x}Mn_xAs compared to the average distance between the manganese ions. The in-plane spin reorientation occurs via the nucleation of 90° domains and rapid domain wall motion^{6,14}, as observed in Fe/Pd superlattices.¹⁶ LKR imaging of magnetic domains motion would allow to check the predictions on dynamics in Ga_{1-x}Mn_xAs films.²¹

IV. CONCLUSION

The magnetization reversal behavior in Ga_{0.957}Mn_{0.043}As films grown on GaAs(001), investigated by independent LKR and MLD measurements, unambiguously demonstrates that the in-plane $\langle 100 \rangle$ directions are the easy magnetization axes. The values of the cubic and uniaxial anisotropies have been determined to be $K_c = 0.75 \times 10^4$ erg/cm³ and K_u

$= 2.32 \times 10^4$ erg/cm³, respectively. The magnetization dynamics in Ga_{1-x}Mn_xAs epilayers looks similar to that found in metallic magnetic films indicating that, in spite of the low Mn concentration, the magnetized state in Ga_{1-x}Mn_xAs is very homogeneous. As recently evidenced,¹⁹ the in-plane spin reorientation occurs via the nucleation of 90° domains and rapid domain wall motion.

ACKNOWLEDGMENT

This work was partly supported, and G. P. M. and M. M. granted, by the European Commission through the Human Potential Program under Contract No. HP-CT-2000-00134, QMDS.

- ¹H. Munekata, H. Ohno, S. Von Molnar, A. Segmüller, L. L. Chang, and L. Esaki, *Phys. Rev. Lett.* **63**, 1849 (1989).
- ²H. Ohno, H. Munekata, T. Penny, S. von Molnár, and L. L. Chang, *Phys. Rev. Lett.* **68**, 2664 (1992).
- ³H. Ohno, A. Shen, F. Matsukura, A. Oiwa, A. Endo, S. Katsumoto, and Y. Iye, *Appl. Phys. Lett.* **69**, 363 (1996).
- ⁴T. Dietl, H. Ohno, and F. Matsukura, *Phys. Rev. B* **63**, 195 205 (2001).
- ⁵F. Matsukura, H. Ohno, A. Shen, and Y. Sugawara, *Phys. Rev. B* **57**, R2037 (1998).
- ⁶Y. Higo, H. Shimizu, and M. Tanaka, *J. Appl. Phys.* **89**, 6745 (2001).
- ⁷A. G. Petukhov, A. N. Chantis, and D. O. Demchenko, *Phys. Rev. Lett.* **89**, 107 205 (2002).
- ⁸M. Tanaka, *J. Vac. Sci. Technol. B* **16**, 2267 (1998).
- ⁹H. Ohno and F. Matsukura, *Solid State Commun.* **117**, 179 (2001).
- ¹⁰D. Hrabovsky, E. Vanelle, A. R. Fert, D. S. Yee, J. P. Redoules, J. Sadowski, J. Kanski, and L. Ilver, *Appl. Phys. Lett.* **81**, 2806 (2002).
- ¹¹K. Sato, *Jpn. J. Appl. Phys.* **20**, 2403 (1981).
- ¹²K. Postava, J. Pistora, D. Ciprian, D. Hrabovsky, M. Lesnak, and A. R. Fert, *Proc. SPIE* **3820**, 412 (1999).
- ¹³J. Ferré and G. A. Gehring, *Rep. Prog. Phys.* **47**, 513 (1984).
- ¹⁴R. P. Cowburn, S. Gray, J. Ferré, J. A. C. Bland, and J. Miltat, *J. Appl. Phys.* **78**, 7210 (1995).
- ¹⁵X. Liu, Y. Sasaki, and J. K. Furdyna, *Phys. Rev. B* **67**, 205 204 (2003).
- ¹⁶J. R. Childress, R. Kergoat, O. Durand, J.-M. George, P. Galtier, J. Miltat, and A. Schuhl, *J. Magn. Magn. Mater.* **130**, 13 (1994).
- ¹⁷K. Postava, H. Jaffres, A. Schuhl, F. Nguyen Van Dau, M. Goiran, and A. R. Fert, *J. Magn. Magn. Mater.* **172**, 199 (1997).
- ¹⁸J. Ferré, in *Spin Dynamics in Confined Magnetic Structures I*, Topics in Applied Physics, Vol. 83, edited by B. Hillebrands and K. Ounadjela, (Springer-Verlag, Berlin, 2002), p. 127.
- ¹⁹U. Welp, V. K. Vlascko-Vlasov, X. Liu, J. K. Furdyna, and T. Wojkovicz, *Phys. Rev. Lett.* **90**, 167 206 (2003).
- ²⁰T. Hayashi, S. Katsumoto, Y. Hashimoto, A. Endo, M. Kawamura, M. Zalautdinov, and Y. Iye, *Physica A* **175**, 284 (2000).
- ²¹T. Dietl, J. König, and A. H. MacDonald, *Phys. Rev. B* **64**, 241 201R (2001).